

## Supporting Information

# 2D-Dual-Spacing Channel Membranes for High Performance Organic Solvent Nanofiltration

*Shaofei Wang, Dinesh Mahalingam, Burhannudin Sutisna, Suzana P. Nunes\**.

Biological and Environmental Science and Engineering Division (BESE), Advanced Membranes and Porous Materials Center (AMPM), King Abdullah University of Science and Technology (KAUST), Thuwal, 23955-6900, Saudi Arabia

\*Corresponding author: Suzana P Nunes, E-mail: [suzana.nunes@kaust.edu.sa](mailto:suzana.nunes@kaust.edu.sa)

## Supplementary Figures

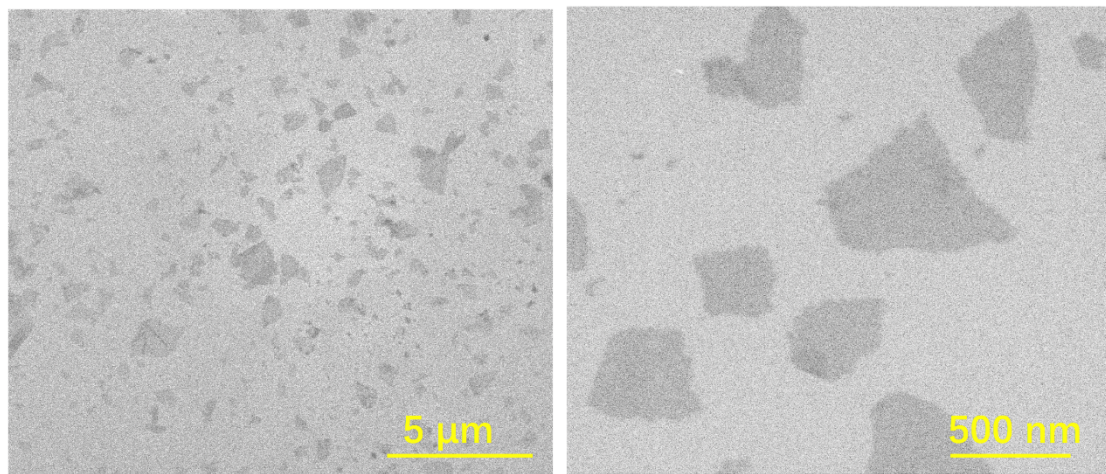


**Figure S1.** SEM images of monolayered GO with different magnifications, showing the lateral size of the GO sheets.

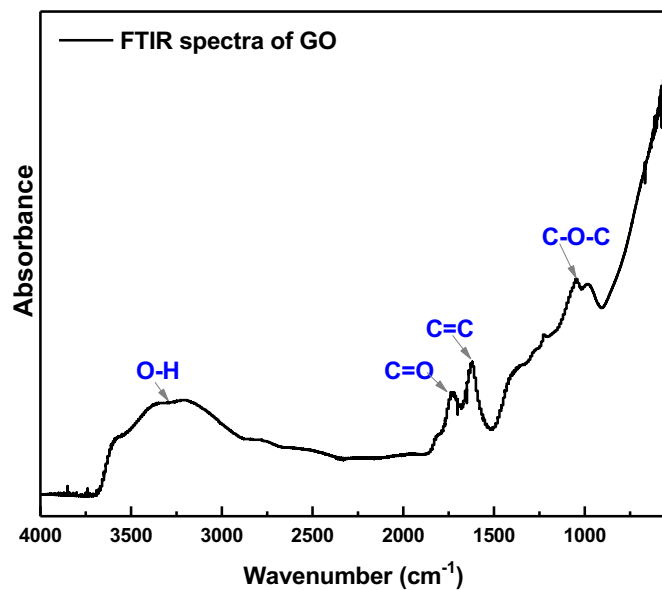


**Figure S2.** FTIR spectrum of GO. The characteristic peaks, O-H stretching vibration at 3420 cm<sup>-1</sup>, C=O stretching vibration of unoxidized sp<sup>2</sup> C-C bonds at 1720 cm<sup>-1</sup> and C-O stretching vibration at 1040 cm<sup>-1</sup>, confirm the oxidation of graphite, which is in accordance with the literature.<sup>1</sup>

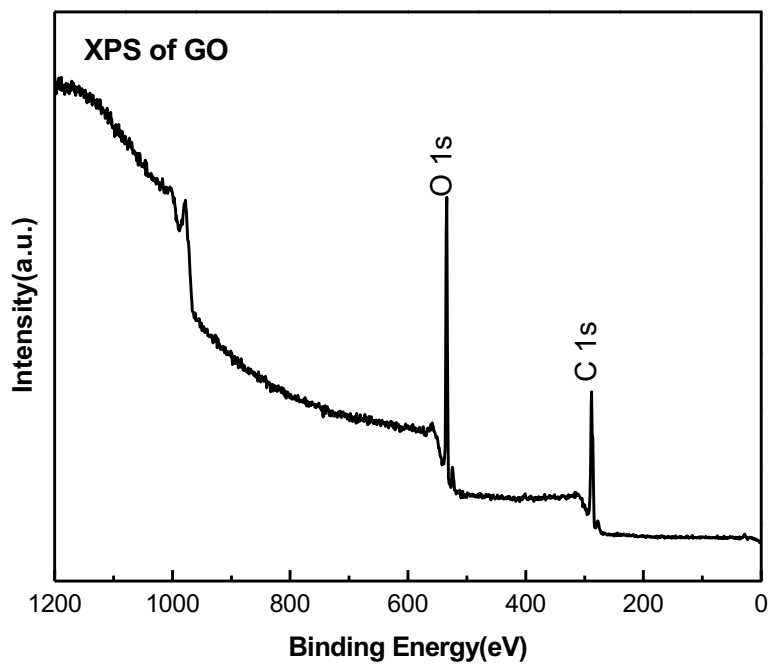


**Figure S3.** XPS analysis of the pristine GO. The C/O atom ratio is about 7/3.

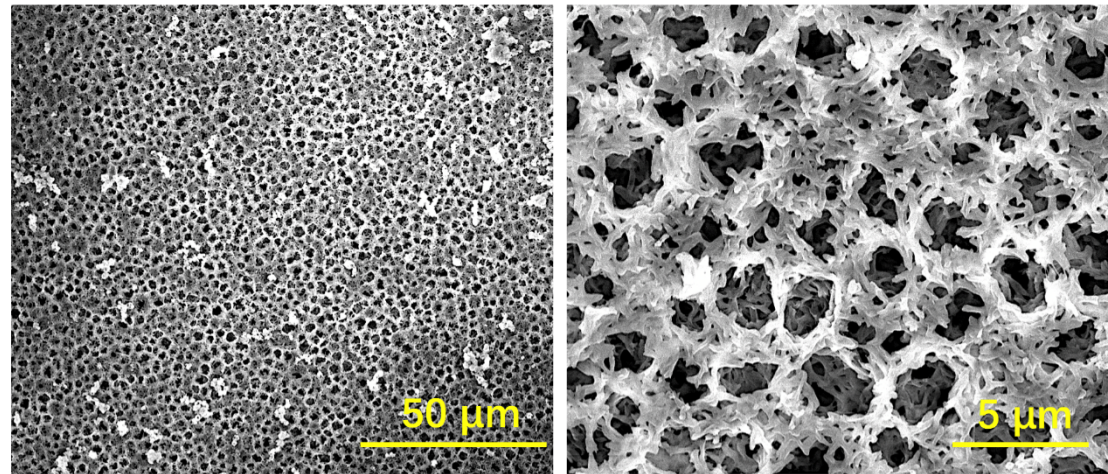


**Figure S4.** SEM images of the surface of the nylon support in different magnifications, showing a highly porous structure with uniform pores size ~0.22 μm.

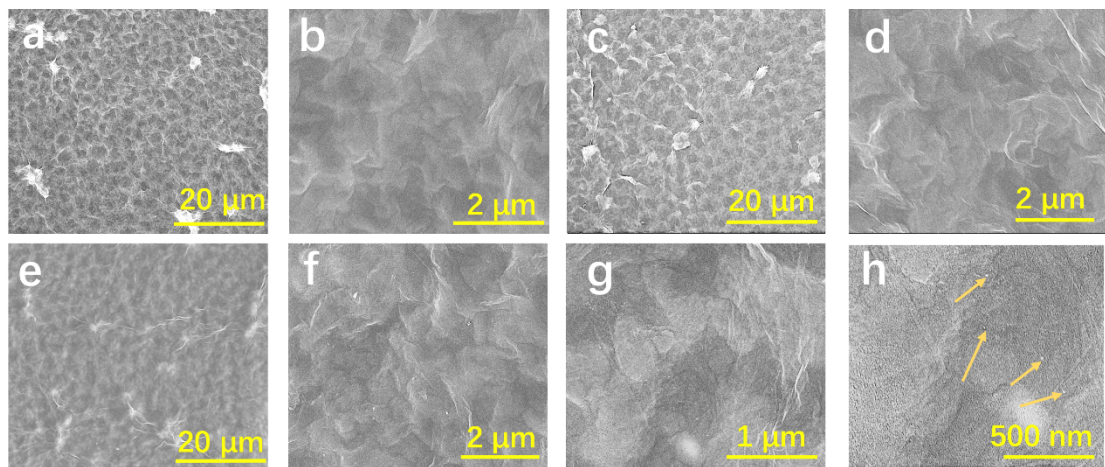


**Figure S5.** SEM images of the surface of membranes prepared with GO loading of  $440 \text{ mg/m}^2$ .

a) and b) pristine GO membranes. c) and d) GO-Si1 membranes. e)-h) GO-Si2 membranes.

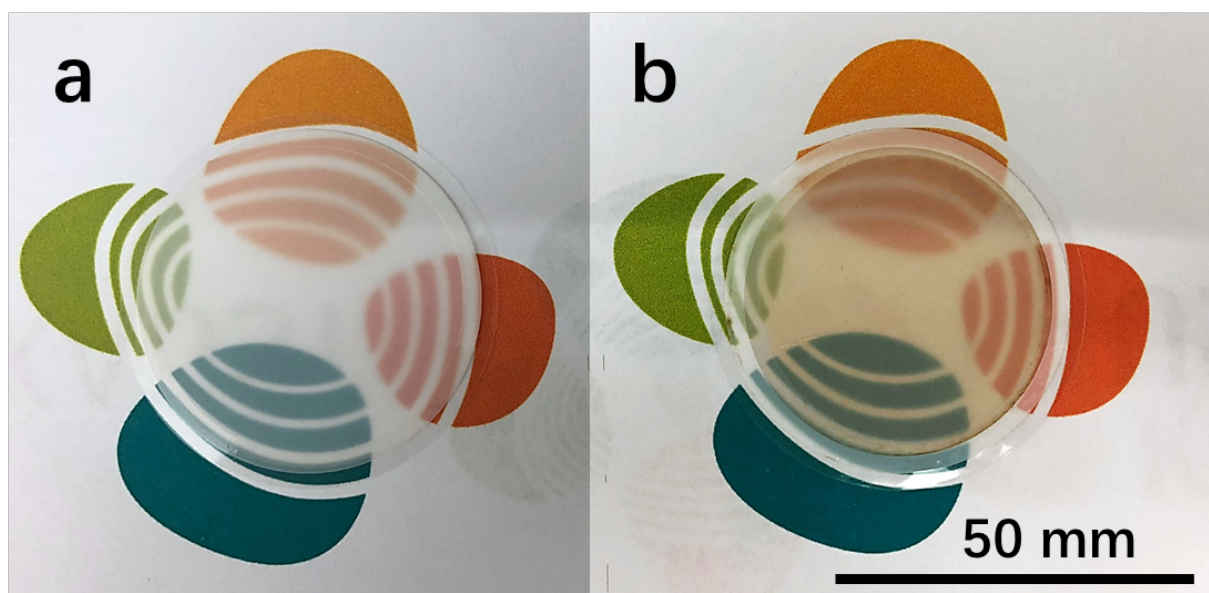


**Figure S6.** Photograph of a) Anodic aluminum oxide (AAO) membrane; b) GO-Si2 membrane on AAO.

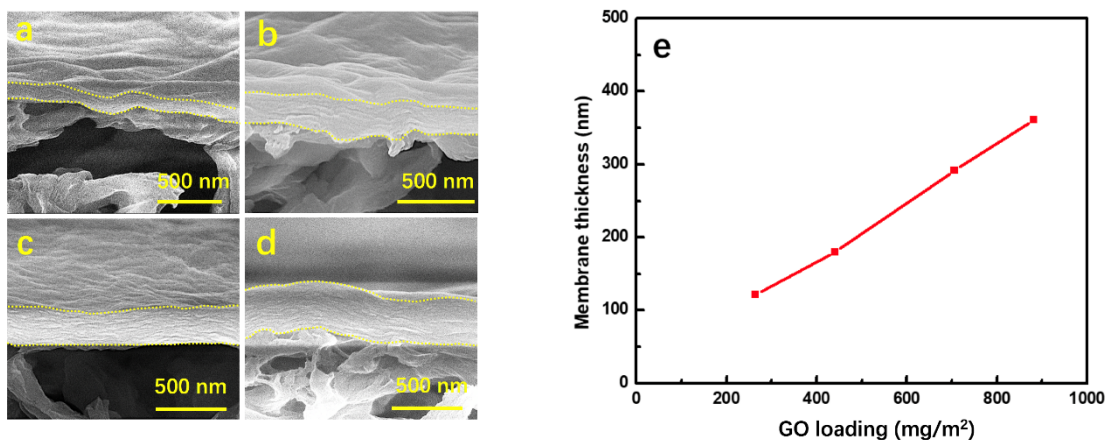


**Figure S7.** a)-d) Cross-sectional SEM image of GO-Si2 membranes with GO loading of 265, 440, 706 and 882 mg/m<sup>2</sup>, respectively. e) Plot of membrane thickness vs GO loading, showing a practically linear relationship.

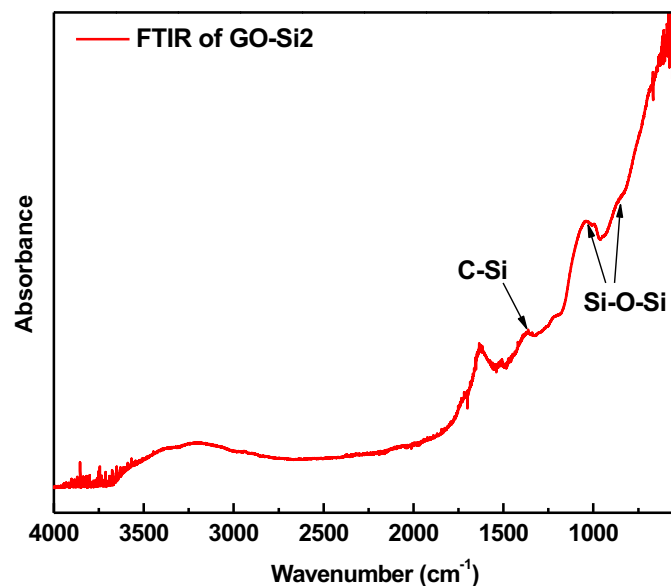


**Figure S8.** FTIR-ATR spectrum of the GO-Si2 membrane.

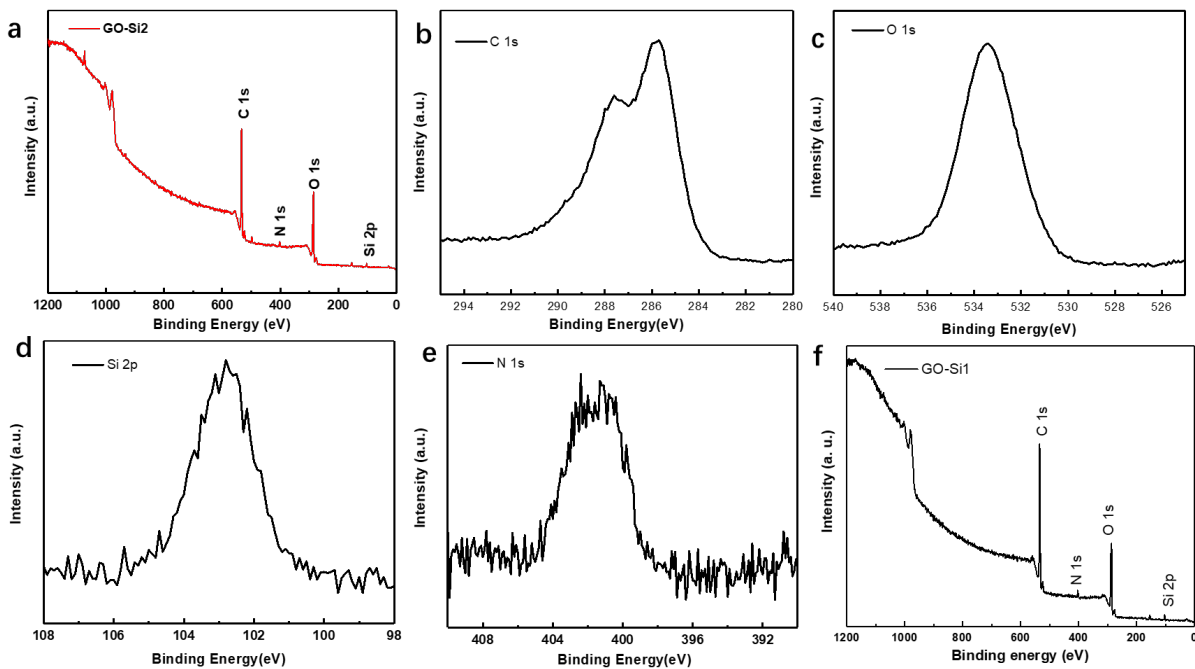


**Figure S9.** XPS analysis of GO-Si membranes. a) Overall XPS spectra of GO-Si2 membrane; b) C 1s, c) O 1s, d) Si 2p and e) N 1s expanded regions of GO-Si2 membrane. The calculated atomic ratio of C/O/Si/N is 66.18/25.45/4.35/4.02 %. f) Overall XPS spectra of GO-Si1 membrane. The Si atom ratio is calculated as 8.63%.

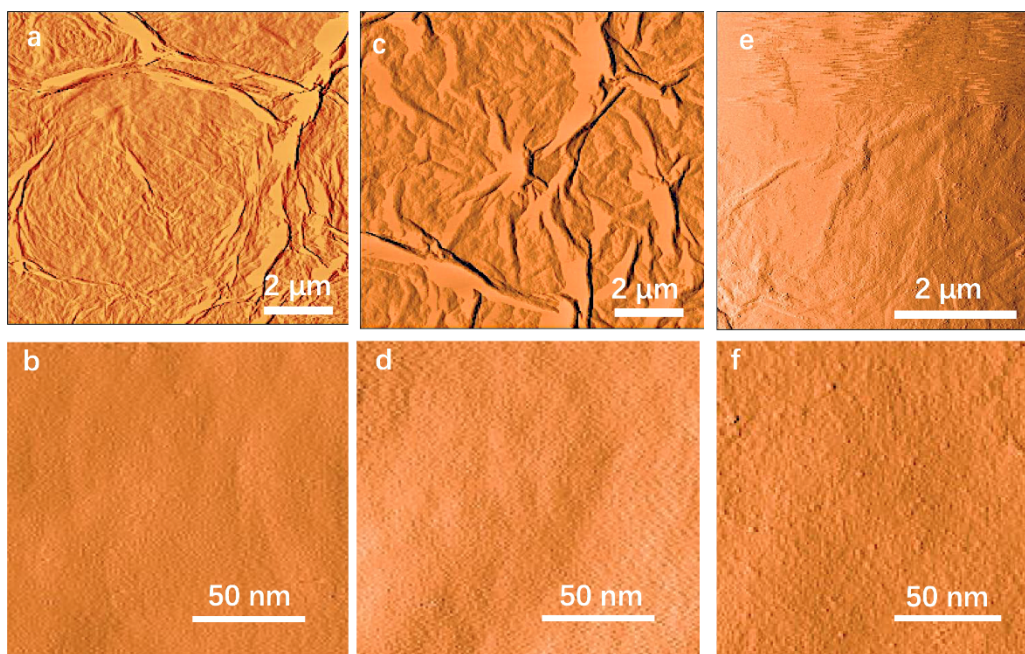


**Figure S10.** AFM images of the membrane surfaces: a) and b) pristine GO membrane, c) and d) GO-Si1 membrane, e) and f) GO-Si2 membrane.

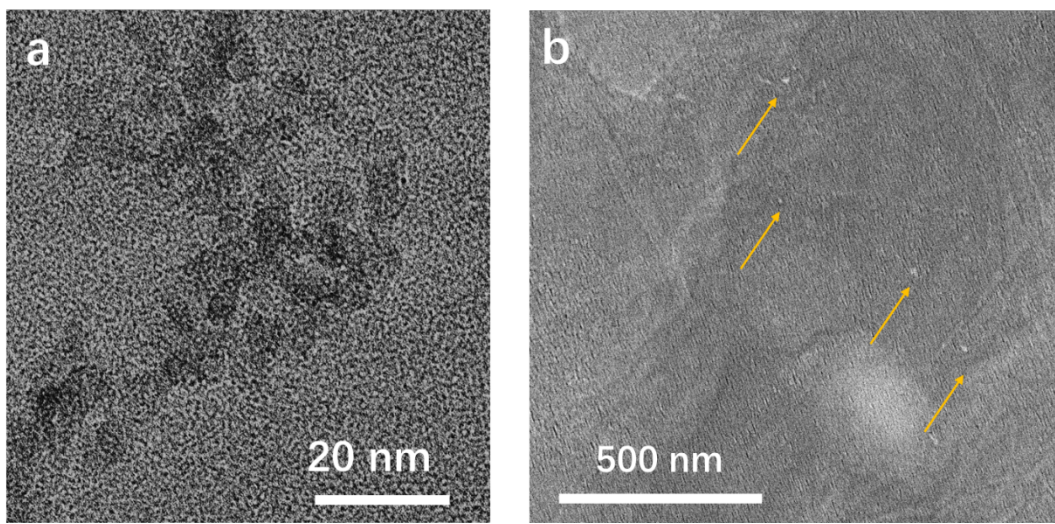


**Figure S11.** Detailed morphology with high magnification electron microscopy images. a) TEM image of a GO-Si2 membrane. b) SEM image of a GO-Si membrane. Arrows demonstrate the location of SiO<sub>2</sub> nanoparticles.

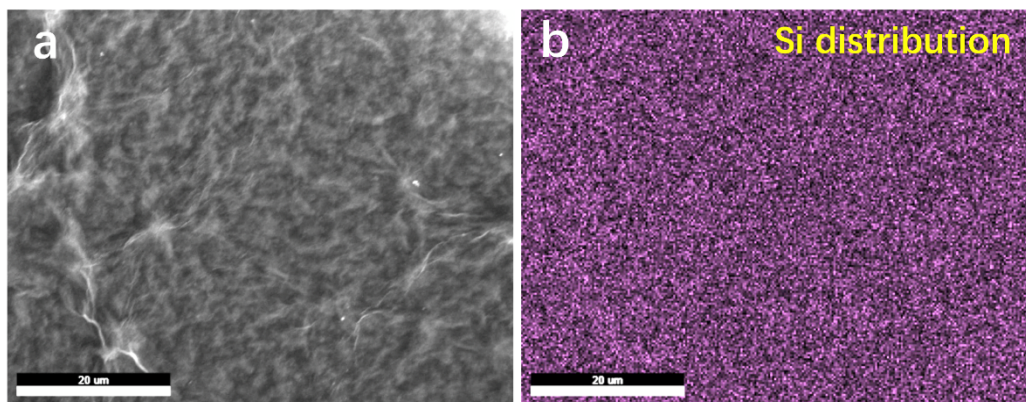


**Figure S12.** Nanoparticles distribution. a) Secondary electrons SEM image of the GO-Si2 membrane surface. b) The Si distribution of image a), by EDS element mapping.

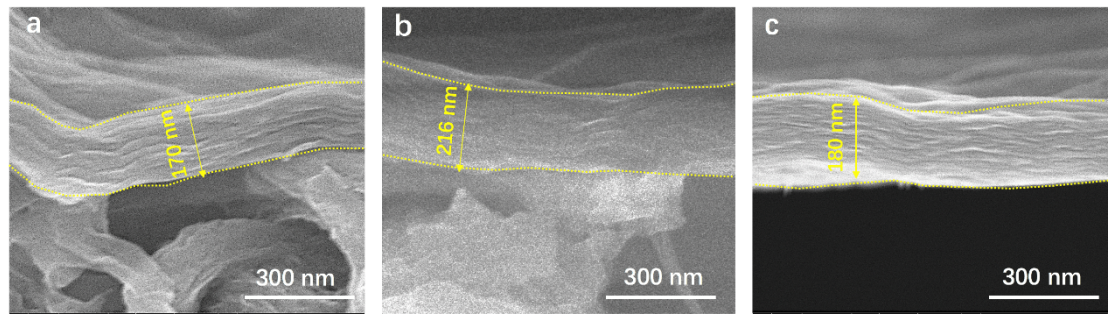


**Figure S13.** Cross-sectional SEM of a) GO, b) GO-Si1 and c) GO-Si2 membranes with the same GO loading.

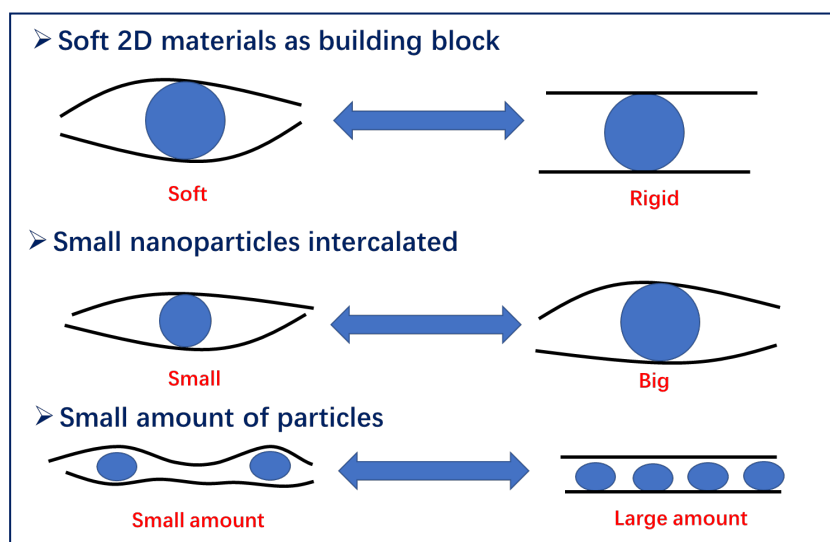


**Figure S14.** Schematic diagram showing the requirements for achieving the dual-spacing nanochannel structure. These requirements may include: using soft 2D materials as building blocks, using small size nanoparticles, with diluted distribution.

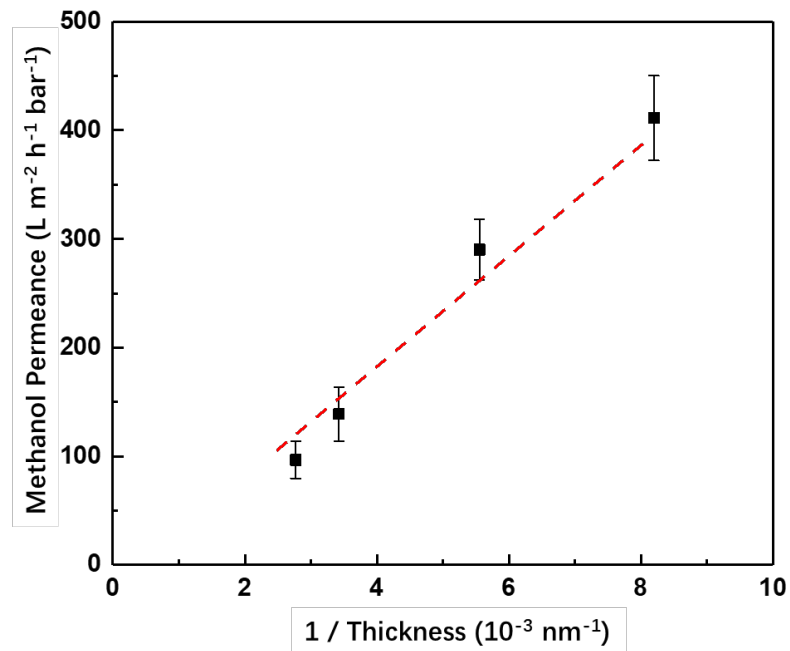
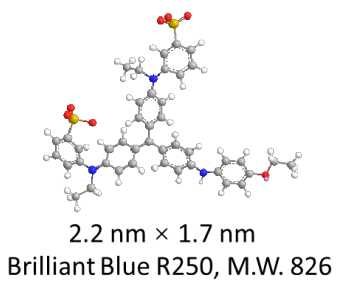
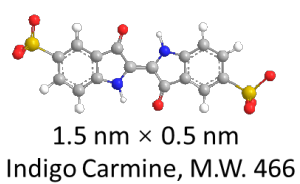
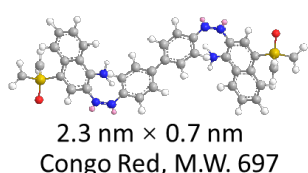
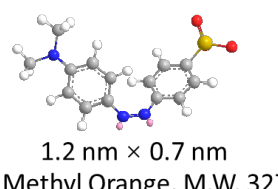


**Figure S15.** Linear correlation between methanol permeance and 1/thickness of the GO-Si2 membrane.

### Negatively charged dyes



### Positively charged dyes

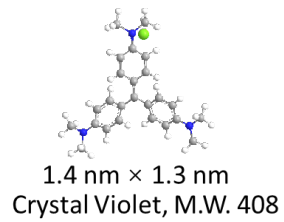
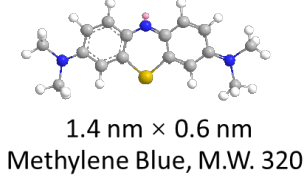
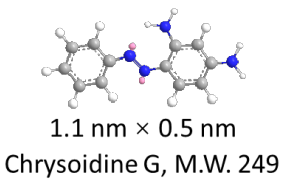


**Figure S16.** Chemical structures of the dyes used for the molecular separation experiments.

The molecular sizes were simulated and estimated, using the Molecular Mechanics 2 method in Chem3D.

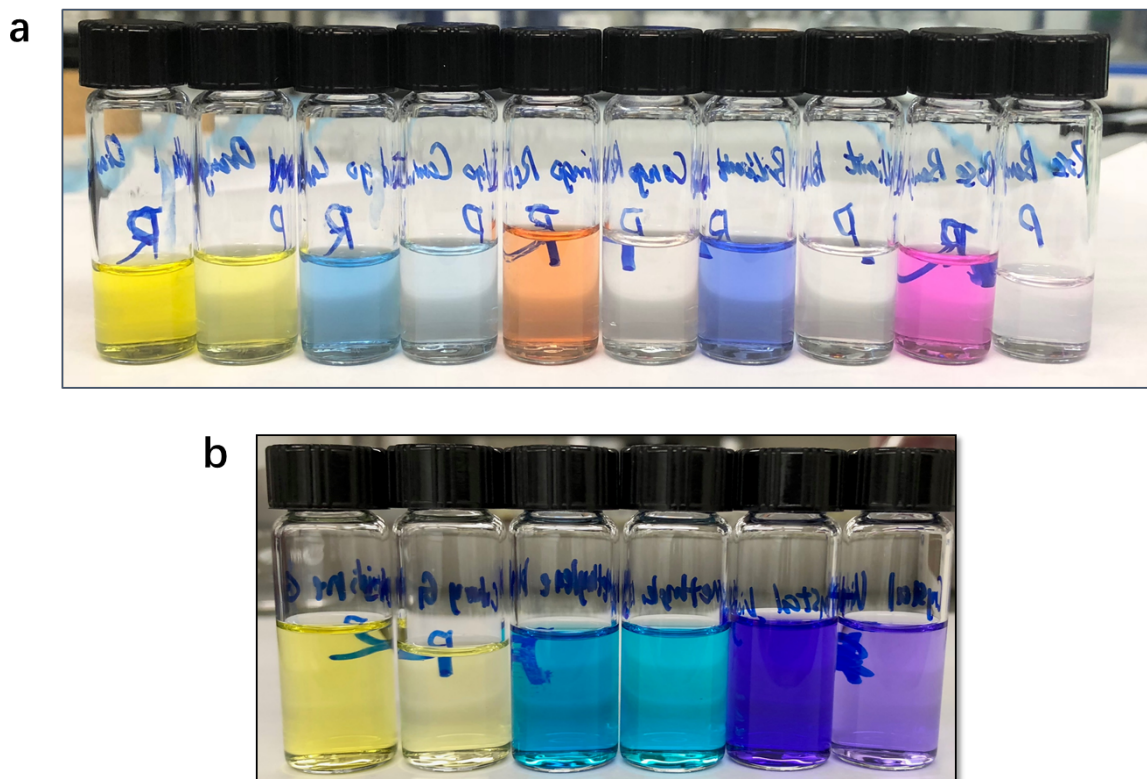


**Figure S17.** Photograph of the feed and permeate solutions with different dyes. a) Negatively charged dyes. From left to right, feed and permeate of methyl orange, indigo carmine, congo red, brilliant blue R250, rose Bengal. b) Positively charged dyes. From left to right, feed and permeate of chrysoidine G, methylene blue, crystal violet.

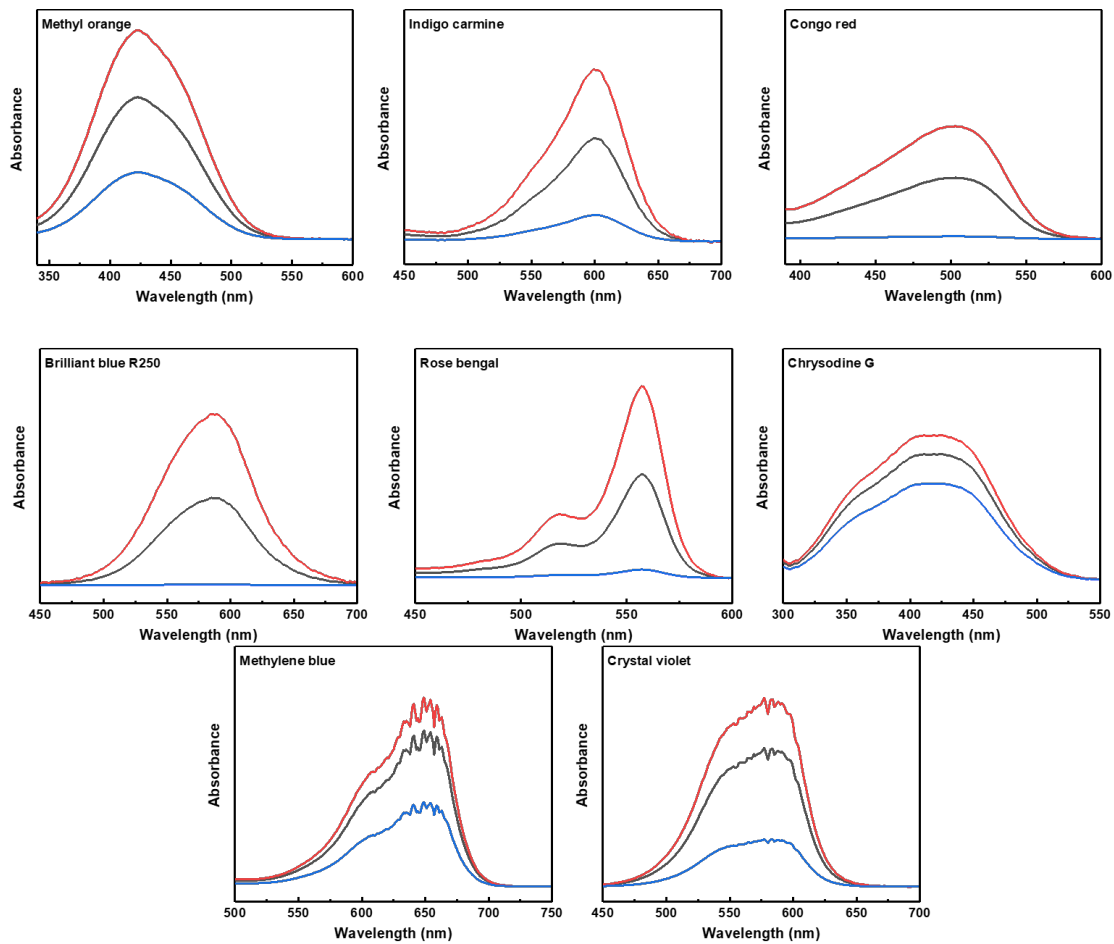


**Figure S18.** UV-vis absorption spectra of the feed (black), retentate (red) and permeate (blue) of different dye methanol solutions from rejection test.

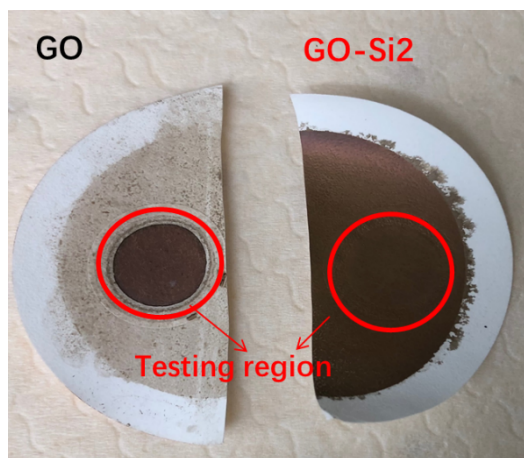


**Figure S19.** Photograph of membranes after 72 h testing in methanol. The red circle indicates the testing region.

## Supplementary Tables

**Table S1.** Gas permeation of the membranes

Membrane	Gas Permeance (GPU) <sup>*</sup>		
	CO <sub>2</sub>	CH <sub>4</sub>	N <sub>2</sub>
GO	1731	1976	1666
Si-GO1	4297	4125	3981
Si-GO2	3810	3613	3758

\* GPU, 1 GPU=  $10^{-6}$  cm<sup>3</sup>(STP)/cm<sup>2</sup> s cmHg

Due to the large channel size, the transport of gases take place through the membranes by Knudsen diffusion. Due to the CO<sub>2</sub>-philic surface on GO, the CO<sub>2</sub> permeance is slightly faster than the theoretical values, based only on molecular size. The Si-GO1 and Si-GO2 membranes have almost the double gas permeance for all gases, which is explained by the expanded interlayer spacings. The Si-GO2 membrane the nanoparticles expand only a few localized parts of the GO layer. In the Si-GO1 membrane, the APTES molecules are homogeneously distributed, expanding the whole interlayer.

**Table S2.** Solvent properties: viscosity, relative polarity, kinetic diameter, and total Hansen solubility parameter.

Solvents	Viscosity at 25°C (mPa S) <sup>2</sup>	Relative polarity <sup>3, 4</sup>	Kinetic diameter (nm) <sup>2</sup>	Total Hansen solubility parameter <sup>2</sup>
acetone	0.310	0.355	0.47	14.9
tetrahydrofuran	0.457	0.207	0.48	19.4
methanol	0.539	0.762	0.38	29.7
dimethylformamide	0.816	0.386	0.50	24.8
water	0.916	1	0.26	47.8
ethanol	1.081	0.654	0.44	26.6
N-methyl-2-pyrrolidone	1.650	0.36	-	22.9
isopropanol	2.058	0.546	0.47	24.6
butanol	2.573	0.586	0.50	23.1

**Table S3.** Rejection and the Cr/Cf values of different dyes.

Dye	Rejection (%)	Cr/Cf <sup>a</sup>	
		Theoretical value <sup>b</sup>	Actual value <sup>c</sup>
Methyl orange	52.7	1.53	1.47
Indigo carmine	74.5	1.74	1.67
Congo red	95.8	1.96	1.84
Brilliant blue R250	99.2	1.99	1.96
Rose bengal	91.9	1.92	1.85
Chrysodine G	23.3	1.23	1.15
Methylene blue	45.8	1.46	1.21
Crystal violet	65.7	1.66	1.36

a. Cr, dye concentration of the retentate. Cf, dye concentration of the feed. b. The theoretical value is calculated assuming that the dye absorption did not occur. c. Actual value obtained from the UV-vis measurement.

**Table S4.** Comparison of the filtration performance of various membranes in methanol.

Membrane	Thickness (nm)	Probe molecule	Methanol		Reference
			permeance (L m <sup>-2</sup> h <sup>-1</sup> bar <sup>-1</sup> ) <sup>1)</sup>	Rejection (%)	
GO-Si2	180	Brilliant blue	290.1	99.2	This work
S-rGO	18	Acid fuchsin	78	70.1	5
HPEI/S-rGO	18	Methylene blue	72.5	90	5
MPD-ACT	95	Acid fuchsin	52.22	99.9	6
FBN	2000	Congo red	600	99	7
Acetylene	10	Protoporphyrin-IX	220	>99	8
PBI/HPBI	1500	Methylene blue	2.60	99.2	9
TFC-MPD/PES	-	Polystyrene oligomers (600)	46.0	>99	10
MXene	230	Reactive black	3563	96 <sup>a</sup>	11
TFN-MIL-101(Cr)	60	Polystyrene oligomers (500)	4.2	97	12
β-CD-2.0	>500	Methyl Orange	5.5	91	13
M-TpTD	104 µm	Rose bengal	138	84	14
M-TpBD	290 µm	Rose bengal	106	99	14
TETA-TFN	-	Crystal violet	27.8	92	15
rGO-TMPyP1.3	36.2	Evans blue	13.0	93	16
HLGO	8	Brilliant blue	7.5	~100	3
PAR-BHPF/PI	20	Rose bengal	8	99	17
TFN	50-120	Tetracycline	20	99	18
CMP	42	Protoporphyrin-IX	22	100	19
Tp-Bpy	2.1 µm	Brilliant blue	108	94	20
PBI/GO	325 nm	Mepenzolate	17	99	21
GO/BA	60 nm	Acid fuchsin	3.5	95	22
Porphyrin/MPD	-	Brilliant blue	32.5	59	23

<sup>a</sup> Rejection was tested in water.

## References

1. D. C. Marcano, D. V. Kosynkin, J. M. Berlin, A. Sinitskii, Z. Sun, A. Slesarev, L. B. Alemany, W. Lu and J. M. Tour, *ACS Nano*, 2010, **4**, 4806-4814.
2. A. Buekenhoudt, F. Bisignano, G. De Luca, P. Vandezande, M. Wouters and K. Verhulst, *J. Membr. Sci.*, 2013, **439**, 36-47.
3. Q. Yang, Y. Su, C. Chi, C. Cherian, K. Huang, V. Kravets, F. Wang, J. Zhang, A. Pratt and A. Grigorenko, *Nat. Mater.*, 2017, **16**, 1198.
4. I. Smallwood, *Handbook of organic solvent properties*, Butterworth-Heinemann, 2012.
5. L. Huang, J. Chen, T. Gao, M. Zhang, Y. Li, L. Dai, L. Qu and G. Shi, *Adv. Mater.*, 2016, **28**, 8669-8674.
6. S. Karan, Z. Jiang and A. G. Livingston, *Science*, 2015, **348**, 1347-1351.
7. C. Chen, J. Wang, D. Liu, C. Yang, Y. Liu, R. S. Ruoff and W. Lei, *Nat. Commun.*, 2018, **9**, 1902.
8. S. Karan, S. Samitsu, X. Peng, K. Kurashima and I. Ichinose, *Science*, 2012, **335**, 444-447.
9. S.-P. Sun, S.-Y. Chan, W. Xing, Y. Wang and T.-S. Chung, *ACS Sustain. Chem. Eng.*, 2015, **3**, 3019-3023.
10. M. F. J. Solomon, Y. Bhole and A. G. Livingston, *J. Membr. Sci.*, 2012, **423**, 371-382.
11. J. Wang, P. Chen, B. Shi, W. Guo, M. Jaroniec and S. Z. Qiao, *Angew. Chem. Int. Ed.*, 2018, **57**, 6814-6818.
12. S. Sorribas, P. Gorgojo, C. Téllez, J. Coronas and A. G. Livingston, *J. Am. Chem. Soc.*, 2013, **135**, 15201-15208.
13. L. F. Villalobos, T. Huang and K. V. Peinemann, *Adv. Mater.*, 2017, **29**, 1606641.
14. S. Kandambeth, B. P. Biswal, H. D. Chaudhari, K. C. Rout, S. Kunjattu H, S. Mitra, S. Karak, A. Das, R. Mukherjee and U. K. Kharul, *Adv. Mater.*, 2017, **29**, 1603945.
15. I. Soroko and A. Livingston, *J. Membr. Sci.*, 2009, **343**, 189-198.
16. T. Gao, L. Huang, C. Li, G. Xu and G. Shi, *Carbon*, 2017, **124**, 263-270.
17. M. F. Jimenez-Solomon, Q. Song, K. E. Jelfs, M. Munoz-Ibanez and A. G. Livingston, *Nat. Mater.*, 2016, **15**, 760-767.
18. X. Guo, D. Liu, T. Han, H. Huang, Q. Yang and C. Zhong, *AICHE J.*, 2017, **63**, 1303-1312.
19. B. Liang, H. Wang, X. Shi, B. Shen, X. He, Z. A. Ghazi, N. A. Khan, H. Sin, A. M. Khattak, L. Li and Z. Tang, *Nat. Chem.*, 2018, **10**, 961-967.
20. K. Dey, M. Pal, K. C. Rout, S. Kunjattu H, A. Das, R. Mukherjee, U. K. Kharul and R. Banerjee, *J. Am. Chem. Soc.*, 2017, **139**, 13083-13091.
21. F. Fei, L. Cseri, G. Szekely and C. F. Blanford, *ACS Appl. Mater. Interfaces*, 2018, **10**, 16140-16147.
22. T. Gao, H. Wu, L. Tao, L. Qu and C. Li, *J. Mater. Chem. A*, 2018, **6**, 19563-19569.
23. P. H. Duong, D. H. Anjum, K.-V. Peinemann and S. P. Nunes, *J. Membr. Sci.*, 2018, **563**, 684-693.